

UC Irvine

UC Irvine Previously Published Works

Title

Transcriptional Mechanisms Link Epithelial Plasticity to Adhesion and Differentiation of Epidermal Progenitor Cells

Permalink

<https://escholarship.org/uc/item/45c8q6vh>

Journal

Developmental Cell, 29(1)

ISSN

1534-5807

Authors

Lee, Briana
Villarreal-Ponce, Alvaro
Fallahi, Magid
[et al.](#)

Publication Date

2014-04-01

DOI

10.1016/j.devcel.2014.03.005

Peer reviewed



Published in final edited form as:

Dev Cell. 2014 April 14; 29(1): 47–58. doi:10.1016/j.devcel.2014.03.005.

Transcriptional mechanisms link epithelial plasticity to adhesion and differentiation of epidermal progenitor cells

Briana Lee¹, Alvaro Villarreal-Ponce¹, Magid Fallahi¹, Jeremy Ovidia², Peng Sun¹, Qian-Chun Yu³, Seiji Ito⁴, Satrajit Sinha⁵, Qing Nie², and Xing Dai^{1,*}

¹Department of Biological Chemistry, School of Medicine, University of California, Irvine, CA, 92697, USA

²Department of Mathematics, University of California, Irvine, CA, 92697, USA

³Department of Pathology and Laboratory Medicine, University of Pennsylvania, Philadelphia, PA 19104, USA

⁴Department of Medical Chemistry, Kansai Medical University, Moriguchi 570-8506, Japan

⁵Department of Biochemistry, State University of New York, Buffalo, NY 14260, USA

Abstract

During epithelial tissue morphogenesis, developmental progenitor cells undergo dynamic adhesive and cytoskeletal remodeling to trigger proliferation and migration. Transcriptional mechanisms that restrict such mild form of epithelial plasticity to maintain lineage-restricted differentiation in committed epithelial tissues are poorly understood. Here we report that simultaneous ablation of transcriptional repressor-encoding *Ovol1* and *Ovol2* results in expansion and blocked terminal differentiation of embryonic epidermal progenitor cells. Conversely, mice overexpressing *Ovol2* in their skin epithelia exhibit precocious differentiation accompanied by smaller progenitor cell compartments. We show that *Ovol1/2*-deficient epidermal cells fail to undertake α -catenin-driven actin cytoskeletal reorganization and adhesive maturation, and exhibit changes that resemble epithelial-to-mesenchymal transition (EMT). Remarkably, these alterations as well as defective terminal differentiation are reversed upon depletion of EMT-promoting transcriptional factor Zeb1. Collectively, our findings reveal *Ovol*-Zeb1- α -catenin sequential repression and highlight functions of *Ovol* as gatekeepers of epithelial adhesion and differentiation by inhibiting progenitor-like traits and epithelial plasticity.

Keywords

Ovol1; *Ovol2*; skin; epidermis/progenitor cells; cell adhesion; epithelial-to-mesenchymal transition (EMT); Zeb1; α -catenin

*To whom correspondence should be addressed: Department of Biological Chemistry, School of Medicine, D250 Med Sci I, University of California, Irvine, CA 92697-1700, Tel: 949-824-3101, Fax: 949-824-2688, xdai@uci.edu.

CONFLICT OF INTEREST

None.

INTRODUCTION

A fundamental question in developmental biology is how epithelial cells maintain dynamic yet stable intercellular adhesions to support tissue morphogenesis (Maiden and Hardin, 2011). Mammalian skin epithelia offer a prime model system to address this. The epidermis and its associated appendages (e.g., hair follicle or HF) develop from a single-layered surface ectoderm during embryogenesis (Koster et al., 2007). Following commitment, epidermal basal cells either differentiate, delaminate, and migrate up to become suprabasal cells, or divide asymmetrically to produce a proliferative daughter cell that remains basal and a transiently proliferative spinous cell that assumes a suprabasal location (Fuchs, 2008). In upward movement, spinous cells differentiate into granular keratinocytes, which go on to produce the outermost stratum corneum constituting a vital permeability barrier. Like-wise, committed HF cells undergo expansion, sorting, first downward and then upward migration on their journey to produce a hair shaft (Jamora and Fuchs, 2002). Epidermal and HF stem/progenitor cells face the challenging need of dampening intercellular adhesions to promote proliferation and migration while achieving stable cell-cell contacts upon tissue maturation (Fuchs, 2007). Adherens junctions and their associated proteins such as E-cadherin (Ecad) and α -catenin lie at the heart of these dynamics (Fuchs and Nowak, 2008). Consistently, ablation of *Cdh1* (Ecad) or *Ctnn1* (α -catenin) in the epidermis results in abnormal intercellular adhesion, hyperproliferation, and altered differentiation (Tinkle et al., 2004; Vasioukhin et al., 2001; Vasioukhin et al., 2000). The resulting defects are significantly more dramatic for the loss of α -catenin, in keeping with its central role in integrating cell adhesion and actin cytoskeleton dynamics with growth signaling (Maiden and Hardin, 2011). To date, transcriptional mechanisms regulating adherens junction proteins have been largely focused on Ecad, whereas the regulation of α -catenin has been thought to occur through genetic mutations and/or post-translational mechanisms (Kobielak and Fuchs, 2004).

Interesting parallels exist between the afore-described developmental epithelial plasticity in skin and the process of epithelial-to-mesenchymal transition (EMT) (Jamora and Fuchs, 2002; Kalluri and Weinberg, 2009). During EMT, epithelial cells lose cell-cell junctions and apical-basal polarity, reorganize their cytoskeleton and shape, gain increased motility, and become mesenchymal cell types. Central to promoting the EMT program are transcription factors of the Snail, Twist and Zeb families (Thiery et al., 2009; Yang and Weinberg, 2008). Developing skin epithelia express EMT-promoting factors: Snail is transiently expressed in HF primordia, and Slug is expressed in embryonic epidermal basal cells (Jamora et al., 2005; Shirley et al., 2010). *K14* promoter-directed overexpression of Snail results in epidermal hyperproliferation and downregulation of Ecad (Jamora et al., 2005), whereas *Slug* null mice show delayed HF development and a thinner epidermis (Shirley et al., 2010). Whether these EMT factors act by promoting physiological adhesive and cytoskeletal remodeling during morphogenesis remains to be demonstrated. More importantly, the molecular mechanism that restricts developmental epithelial plasticity to ensure coordinated proliferation and differentiation of skin epithelial progenitor cells are complete unknowns.

The Ovo family of zinc-finger transcription factors constitutes a downstream hub of signaling pathways including Wg/Wnt, EGF, and BMP/TGF- β (Descargues et al., 2008;

Gomis et al., 2006; Li et al., 2002b; Nair et al., 2006; Payre et al., 1999). *Ovol1* null mice display epithelial anomalies including mildly hyperproliferative epidermis, abnormal hair shafts, defective spermatogenesis, and kidney cysts (Dai et al., 1998; Li et al., 2005; Nair et al., 2006; Teng et al., 2007), whereas *Ovol2* null mice die during mid-gestation (Mackay et al., 2006). In this work, we report studies that uncover compensatory/redundant roles of *Ovol1* and *Ovol2* as negative regulators of a progenitor cell state and positive regulators of terminal differentiation in at least two skin epithelial lineages, interfollicular epidermis and HFs. Moreover, we provide compelling evidence that *Ovol1/2* promote the differentiation of epidermal progenitor cells in part by inhibiting EMT pathway components such as *Zeb1*, which in turn represses *Ctnn1* (α -catenin) transcription. These findings open the door to understand the molecular control of developmental epithelial plasticity and epidermal differentiation by studying the involvement of other classical EMT regulators.

RESULTS

Simultaneous ablation of *Ovol1* and *Ovol2* results in defective maturation of embryonic epidermis and HFs

In addition to *Ovol1* (Li et al., 2002a; Nair et al., 2006), *Ovol2* is also expressed in epidermal and HF progenitor cells as they mature during embryogenesis. Nuclear *Ovol2* is present predominantly in basal but also a few suprabasal epidermal cells, as well as in the down-growing front of developing HFs (Figure 1A). When epidermal cells were laser captured for RNA analysis, a significant increase in *Ovol2* mRNA was seen from E13.5 and E16.5 (Figure 1B). To investigate *Ovol2* function in skin, we generated skin epithelia-specific *Ovol2* knockout (SSKO: *Ovol2*^{f/f}/*K14-Cre*) mice (Figure S1A). These mice developed normally, with their skin exhibiting no remarkable morphological or biochemical defects (Figure S1B–C), but showing dramatically elevated level of *Ovol1* mRNA, especially in basal keratinocytes (Figure S1D, S1E). These findings, together with our previous observation of elevated *Ovol2* expression in *Ovol1*-deficient epidermis (Teng et al., 2007), raise the possibility of compensation/redundancy between *Ovol1* and *Ovol2*.

To address this, we generated *Ovol1/2* double knockout (DKO: *Ovol1*^{-/-}/*Ovol2*^{f/f}/*K14-Cre*) mice. Like *Ovol1*^{-/-} (Nair et al., 2006), DKO embryonic epidermis contained an expanded K1-positive spinous compartment (Figure 1C–D). Moreover, DKO epidermis displayed a number of features not observed in *Ovol1*^{-/-}. First, K5/K14/K15-positive cells expanded beyond the basal compartment, especially at earlier stages of development (Figure 1E–F and data not shown). Second, cells throughout the basal and spinous layers displayed abnormal morphology and shape, and were often separated by notable intercellular spaces (Figures 1C, S1F). Third, the granules and cornified layers appeared immature, defects most prominently evident in electron microscopic (EM) and semi-thin images (Figures 1G, S1F). Consistently, the levels of late differentiation markers involucrin and filaggrin were decreased (Figure S1G). Finally, DKO epidermis failed to shed the K15-positive periderm when stratification should be complete (Figure 1C, F). In keeping with these maturation defects, DKO embryos lacked a functional permeability barrier, as illustrated by persistent dye penetration (Byrne et al., 1994) beyond E17.5 (Figure 1H).

HF in DKO embryos also failed to mature properly. Compared to counterparts in control and *Ovol1*^{-/-} skin, DKO HF were smaller (Figure 1I) and their length was decreased (Figure 1J). Moreover, the number of HF that express AE13, a hair keratin marker of the differentiating precortex/cortex cells, was decreased (Figure 1K). Collectively, our data reveal compensatory/redundant roles of *Ovol1* and *Ovol2* in restricting the size of the basal/spinous compartments, and in facilitating terminal differentiation within both interfollicular epidermal and HF lineages.

Loss of *Ovol1/2* leads to increased basal cell proliferation and expanded progenitor cell marker expression

Next we asked whether the expanded basal compartment in DKO epidermis associates with increased proliferation, by quantifying the number of phospho-histone H3 (pH3)-positive mitotic cells. Compared to control and *Ovol1*^{-/-}, DKO epidermis contained a higher number of mitotic cells in the basal layer (Figure 2A). To assess whether *Ovol1/2* play a keratinocyte-autonomous role in basal cell proliferation, we cultured primary keratinocytes from E18.5 DKO and control embryos in low-Ca²⁺ medium, which mimics the basal state. DKO keratinocytes grew more rapidly and reached confluence faster than control and *Ovol1*^{-/-} cells (data not shown). When plated at a clonal density, DKO and *Ovol1*^{-/-} keratinocytes produced a significantly higher number of colonies than control (Figure 2B). Thus, reducing *Ovol* dosage in basal cells leads them to display enhanced proliferation potential. Interestingly, while control and *Ovol1*^{-/-} colonies were darkly stained with dye, reflecting a tightly packed morphology, DKO colonies were large, loose clusters of cells that were weakly stained (Figure 2B). We will return to this issue later.

To probe the underlying molecular defects, we compared gene expression between control and DKO primary keratinocytes. Consistent with known *Ovol1/OVOL2* regulation of *Myc/MYC* (Nair et al., 2006; Wells et al., 2009), Gene Set Enrichment Analysis (GSEA) (Mootha et al., 2003) of microarray data revealed an enrichment of a MYC-activated gene set (Zeller et al., 2003) in DKO cells compared to control (Figure S2A). Interestingly, DKO cells also displayed an enrichment of three “stemness” gene sets (Figure S2B). MYC target and “stemness” gene sets were still enriched when proliferation/cell cycle genes were removed from the analysis (Figure S2C–D), indicating that the enrichment was not solely due to increased proliferation. Among the enriched “stemness” genes was *Trp63* (p63), which encodes a self-renewal factor previously shown to be a master regulator of epidermal morphogenesis (Mills et al., 1999; Yang et al., 1999). RT-PCR confirmed elevated expression of *Np63* (Figure S2E). Moreover, while nuclear p63 is normally restricted to the basal layer, it was detected not only strongly in basal but also in many suprabasal cells in DKO epidermis (Figure 2C). Sequence analysis revealed 5 putative *Ovol* binding sites in *Np63* promoter (Figure 2D). In chromatin immunoprecipitation (ChIP) assays, *Ovol2* bound to both *Np63* and *Myc* promoters in primary keratinocytes at the predicted sites (Figure 2D). Thus, in addition to *Myc*, *Np63* is likely a direct target of *Ovol2*.

GSEA also revealed enrichment in DKO cells of gene sets previously shown to be enriched in adult HF bulge stem cells (HF-SCs) (Lien et al., 2011) (Figure S2F). Remarkably, a quarter (24%) of the HF-SC signature was affected by *Ovol1/2* loss (Figure S2G). An

enrichment of a basal cell carcinomas gene set was also observed (Figure S2H). Among the enriched HF-SC genes were those encoding K15 and Tcf3, which normally are also expressed in embryonic epidermal basal cells (Nguyen et al., 2006; Romano et al., 2010). We observed ectopic K15-positive cells, especially at early embryonic stages, and a persistent presence of Tcf3 in suprabasal cells in DKO epidermis (Figures 1F, 2E and data not shown). In contrast, the expression of several HF-specific/enriched stem cell markers, including Lrig1, Sox9, Nfatc1, and CD34 (Woo and Oro, 2011), did not exhibit any difference between control and DKO skin (Figure S3 and data not shown). Collectively, these data suggest that loss of *Ovol1/2* results in an enhancement of molecular features associated with a primitive epidermal progenitor cell state that overlaps but is distinct from a HF-SC state.

Epithelially directed *Ovol2* overexpression results in compromised progenitor cell compartments and premature differentiation in developing skin and adult HFs

To substantiate *Ovol* function in epidermal progenitor cells, we generated *TRE-Ovol2/K5-tTA* bitransgenic (BT) mice. In the absence of doxycycline (Dox), these mice overexpress *Ovol2* in embryonic K5-positive cells, which include the epidermal basal layer and the presumptive ORS of HFs (Byrne et al., 1994; Diamond et al., 2000) (Figure S4A). As *Ovol1* and *Ovol2* recognize nearly identical DNA sequences (Wells et al., 2009), we expect *Ovol2* overexpression to misregulate both *Ovol1* and *Ovol2* targets. BT animals fed on a Dox-free diet displayed a thinner epidermis than their control littermates (Figure 3A) and died shortly after birth. K15 expression was nearly absent (Figure 3B), and the K1-positive spinous compartment was reduced in size (Figure 3A, C). Granular layers and stratum corneum were also smaller but less remarkable (Figure 3A, D and data not shown). Microarray analysis of control and BT embryonic skin revealed a significant downregulation of “stemness” gene sets in the latter (Figure S4B). Further, BT embryonic skin produced dramatically decreased staining for p63 protein (Figure 3E). These alterations suggest reduced epidermal stem/progenitor cells upon *Ovol2* overexpression.

HF morphogenesis was affected in a similar manner. The number of HFs in BT embryos was greatly reduced, and the few residual HFs contained shorter trunks, where presumptive HF stem/progenitor cells likely reside (Nowak et al., 2008) (Figure 3A, B, F). In contrast, the bulbs of the residual HFs appeared largely normal, and expressed proper lineage differentiation markers including AE13, inner root sheath marker *Gata3*, and matrix/precortex marker *Lef1* (Figures 3F, S4C). Thus, aberrantly elevated *Ovol2* expression in embryonic HF epithelial cells diminishes the progenitor cell compartment, while still permitting terminal differentiation.

The molecular similarity between embryonic epidermal progenitor cells and adult HF-SCs (Blanpain and Fuchs, 2009) prompted us to determine whether *Ovol2* overexpression affects the latter. To activate transgene expression only in adult skin (specifically in HF ORS/bulge and epidermal basal cells), BT mice were fed a Dox-containing diet during gestation, and Dox was then removed postnatally at different ages (Figure S4D). Upon *Ovol2* overexpression, adult BT mice displayed a loss of K15-positive cells in both epidermis and HF bulge (Figure 4A). Further, BT HFs displayed reduced expression of *Tcf3* in the bulge

and secondary hair germ (HG) (Figure 4B). In contrast, CD34 expression was not affected (Figure S4E). Prolonged transgene expression resulted in hair loss in older BT mice (Figure 4C), and histological analysis confirmed a near-complete absence of HFs; the epidermis was thickened and the residual HFs were epidermalized as shown by aberrant K1 expression (Figure 4D and data not shown).

Adult HFs undergo cyclic bouts of growth (anagen), regression (catagen) and resting (telogen) (Beck and Blanpain, 2012). Proliferation and differentiation of stem/progenitor cells in the bulge/HG drives telogen to anagen transition. To examine *Ovol2* function in this transition, we activated the *Ovol2* transgene at postnatal (P) day 49, when HFs are normally in the second telogen. At P63, when HFs in WT mice were still in telogen, HFs in BT littermates had progressed to late anagen (Figure 4E). This was not due to chronic effects of leaky transgene expression (Figure S4F). Collectively, our analyses demonstrate that upon *Ovol2* overexpression, adult HFs fail to maintain stem/progenitor cells and undergo precocious differentiation.

***Ovol1/2*-deficient keratinocytes exhibit EMT-like changes ex vivo**

Our studies above highlight a positive role of *Ovol1/2* in epidermal differentiation. To seek additional and alternative mechanisms beyond direct repression of *Myc* and *Np63*, we returned to the comparative expression analysis of control and DKO keratinocytes. Remarkably, the expression of myriad mesenchymal markers such as *Vim* (vimentin or Vim) (15x), *Acta2* (smooth muscle actin or SMA) (10x), *Vcan* (versican) (5x), *Cdh2* (N-cadherin or Ncad) (4x), and *Fnl1* (fibronectin) (3x) was significantly elevated, whereas that of epithelial markers such as *Ocln* (occludin) (18x), *Krt19* (K19) (9x), and *Cdh1* (Ecad) (3x) was significantly reduced in DKO cells (Table S1). RT-PCR confirmed some of these changes (Figure 5A). Moreover, abundant Vim-positive cells, many of which also stained positive for K14, were detected in DKO culture (Figure 5B). The expression of genes encoding EMT-promoting transcription factors, namely *Zeb1* (43x), *Zeb2* (6x), and *Snai2* (Slug) (1.7x), but not *Twist1* and *Snai1*, was dramatically upregulated in DKO cells (Table S1, Figure 5A).

Consistent with EMT-like molecular changes, DKO keratinocytes displayed a tendency to grow as dispersed cells and adopted a fibroblast-like morphology (Figures 2B, 5C). Genotyping revealed near-complete recombination of the floxed *Ovol2* locus (Figure S5A), indicating that these cells were of an epithelial origin. Moreover, DKO cells were significantly more migratory in scratch assays than control (Figure 5D).

Unrestricted epithelial plasticity/EMT may cell-autonomously compromise the differentiation potential of epidermal cells. Indeed, Ca^{2+} induced less remarkable differentiation of DKO cells compared to control (Figure 5E–F). Even in low- Ca^{2+} medium, where control keratinocytes expressed low but appreciable levels of mRNAs of differentiation genes such as members of the transglutaminase (*Tgm*), late cornified envelope (*Lce*), and small proline-rich protein (*Sprp*) families, DKO cells showed significantly reduced expression of these genes (Table S2). Thus, loss of *Ovol1/2* renders keratinocytes intrinsically refractory to Ca^{2+} -induced terminal differentiation.

EMT-like gene expression and abnormal cell adhesion in *Ovol1/2*-deficient epidermis

To determine whether EMT-like changes occur in vivo, we performed quantitative Western blot analysis of freshly isolated embryonic epidermis. Most dramatic elevation was seen for *Zeb1*, *Vim*, and *SMA*, whereas a slight increase was seen for *Ncad* (Figure 6A). While only a few scattered *Zeb1*-positive cells were present at the basal-suprabasal junction of control epidermis, DKO epidermis exhibited abundant presence of such cells in both basal and suprabasal compartments (Figure 6B). Moreover, while occasional *Vim*-positive cells were detected in the control basal layer, almost all DKO basal cells stained positive for *Vim*, albeit at a lower intensity compared to the underlying dermis (Figure 6C). The level of *Vim* and *Zeb1* mRNAs was also significantly increased (Figure 6D), suggesting that their upregulation occurs at a transcriptional level. Intriguingly, the mRNA level and staining pattern of *Ecad*, a well-known *Zeb1* target (Peinado et al., 2007), were unaltered in DKO epidermis (Figures 6A; S5B).

To better understand *Ovol1/2* DKO cellular defects in vivo, we returned to EM analysis. Importantly, while basal and spinous cells in DKO epidermis were able to form intermittent intercellular bridges/filopodia-like structures and normal-looking desmosomal junctions, they failed to properly “zip” together the intervening membranes to maintain full adhesion to one another (Figure 6E). These defects are strikingly similar to mice deficient in α -catenin, which is required for actin cytoskeleton organization to seal adjacent cell membranes during the formation of stable epidermal cell-cell contacts (Vasioukhin et al., 2000). Consistent with this parallel, the level of α -catenin protein was significantly reduced in DKO epidermis (Figure 6A).

The retention of *Ecad* in DKO cells in vivo led us to wonder whether artificially enhancing cell-cell contacts in cultured DKO keratinocytes might suppress their EMT-like changes. To address this, we added Ca^{2+} , which induces intercellular adhesion prior to differentiation (Jamora and Fuchs, 2002), to keratinocyte cultures. Consequently, DKO cells no longer exhibited as significant a deviation from the control in their expression of most EMT-related genes, such as *Cdh2*, *Acta2*, and *Snai2* (Table S1). However, the top-affected genes in low Ca^{2+} , such as *Zeb1* and *Vim*, still showed increased expression in DKO cells, albeit to a lesser extent. Importantly, *Ctnn1* (α -catenin) expression was significantly lower in Ca^{2+} -treated DKO cells than control. From these findings, we surmise that: 1) the presence of rigid cell-cell organization and differentiation cues in vivo might counterbalance the EMT tendency of *Ovol1/2*-deficient epidermal cells; 2) misregulation of *Zeb1*, *Vim*, and *Ctnn1* likely represents primary molecular effects of *Ovol1/2* loss, whereas the additional changes that occur only in culture (e.g., reduced *Cdh1* expression) may be secondary.

Zeb1 mediates *Ovol* regulation of *Ctnn1*, EMT, and terminal differentiation

We next tested the possibility that *Ovol* directly regulate EMT-inducing genes in epidermis. Regulatory regions of *Zeb1*, *Vim* and *Snai2* genes contain *Ovol* binding motifs, and CHIP experiments revealed *Ovol2* binding to the predicted sites in primary keratinocytes (Figure 7A and data not shown). Moreover, the relative binding strength positively correlated with the extent of upregulation in mRNA expression (see above), with *Zeb1* being the most strongly bound and most significantly upregulated. We therefore asked whether depletion of

Zeb1 rescues the defects of DKO keratinocytes. Transfection of a *Zeb1*-specific siRNA, but not a negative control siRNA, into DKO keratinocytes cultured in low Ca^{2+} resulted in efficient *Zeb1* knockdown (Figure S6A), formation of colonies with epithelial morphology (Figure 7B), and correction of *Fn1*, *Cdh2*, and *Cdh1* mRNA expression to near-control levels (Figure 7C). Importantly, *Cttna1* mRNA expression was also restored after *Zeb1* knockdown (Figure 7C).

The inverse correlation between *Zeb1* and *Cttna1* expression led us to examine whether *Cttna1* is a target of *Zeb1* transcriptional repression. Previous ChIP-seq studies (UCSC genome browser) revealed ZEB1 peaks on the human *CTNNA1* promoter (Figure S6B). Our ChIP experiments revealed *Zeb1* binding to the mouse *Cttna1* promoter in primary keratinocytes (Figure 7D). In reporter assays, co-transfection with a *Zeb1* expression construct repressed luciferase activity driven by the *Cttna1* promoter, but not a mutant promoter where the upstream binding site is mutated (Figure 7E). These data establish *Cttna1* as a direct target of *Zeb1*.

Next we asked whether *Zeb1* depletion affects how *Ovol1/2* deletion impacts cell adhesion and actin dynamics of cultured DKO keratinocytes. Shortly after plating, α -catenin protein was concentrated to cell borders of control cells that came into close proximity of each other; over the several days, the cells eventually sealed together with α -catenin staining remaining strongest at the borders (Figure 7F, left). As expected (Vasioukhin et al., 2000), phalloidin staining revealed actin filaments that localized radially at the periphery of control cells: weak right after plating but enhanced over culturing (Figure 7F, left). In contrast, DKO cells did not show appreciable localization of α -catenin to the cell borders even when they were contacting each other, and abundant stress fibers formed in these cells over time (Figure 7F, middle). When *Zeb1* was depleted, α -catenin localization and actin cytoskeletal staining in DKO keratinocytes resembled control cells (Figure 7F, right). No apparent effect was observed when *Zeb1* was depleted in control keratinocytes (data not shown).

Thus, reducing *Zeb1* expression is capable to return *Ovol1/2* DKO keratinocytes to an epithelial state. Is this sufficient to restore their differentiation potential? Indeed, *Zeb1* depletion in DKO keratinocytes led to increased mRNA levels of late epidermal differentiation genes *Tgm1* and *Sprrr2j* (Figure 7C), as well as partially rescued the expression of differentiation markers *Tgm3* and filaggrin (Figure S6C). In contrast, the expression of self-renewal/proliferation genes *Myc*, *Tcf3*, *Krt15* (K15), and *Itga6* ($\alpha 6$ integrin) were not affected (Figure S6D). Interestingly, *Zeb1* knockdown resulted in an increased number of colonies formed by DKO keratinocytes while exerting a minimal effect on control cells (Figure 7G). Collectively, our data suggest a model that *Ovol* proteins maintain the epithelial identity and differentiation competence of epidermal progenitor cells in part via an *Ovol-Zeb1- α -catenin* regulatory pathway.

DISCUSSION

Our work underscores *Ovol1* and *Ovol2* as critically important regulators of epidermal morphogenesis. Overall, they promote terminal differentiation within both epidermal and HF lineages, and restrict molecular stem/progenitor cell traits and proliferation potential.

Importantly, the study uncovers a previously unrecognized mechanism, where a molecular machinery used to regulate epithelial plasticity confers differentiation competence to epidermal progenitor cells.

While *K14-Cre*-mediated deletion of *Ovol2* results in a near complete arrest of mammary morphogenesis (Watanabe et al., submitted), it severely impacts epidermal differentiation only when *Ovol1* is also deleted (this work). In various assays, *Ovol1*^{-/-} skin either displayed a status that is intermediate between control and DKO or was similar to control, whereas *Ovol2* SSKO skin was indistinguishable from the control (Figures 1, S1, 2, S2, and data not shown). *Ovol1* and *Ovol2* are expressed in distinct but overlapping sites of the developing epidermis. It is possible that under physiological conditions, they each regulate the behavior of distinct subpopulations of epidermal progenitor cells. However, when one is absent, the other is up-regulated, reflecting compensatory attempts of the cells to ensure that essential developmental/cellular processes can take place. Proper epidermal differentiation leading to barrier formation is essential for the organism's extra-utero survival. Perhaps for this reason, functional compensation/redundancy between *Ovol1* and *Ovol2* is particularly important in developing epidermal progenitor cells.

Interestingly, both reduction and increase in *Ovol* dosage leads to catastrophic consequences, although for different underlying reasons. For example, DKO embryos produce HFs that contain few AE13-positive cells, whereas BT HFs, when formed, seem to generate AE13-positive cells at the expense of HF progenitor cells. These findings imply the need to exquisitely control total *Ovol* protein levels in skin in order to balance progenitor cell proliferation with differentiation. Both *Ovol1* and *Ovol2* promoters contain *Ovol* binding motifs, and *Ovol1* auto-represses (Nair et al., 2007; Teng et al., 2007; Wells et al., 2009). These findings suggest that *Ovol1* and *Ovol2* may mutually repress each other's expression (and auto-repress) to maintain adequate total levels of *Ovol* proteins.

Both unipotent embryonic epidermal stem/progenitor cells and multipotent adult HF-SCs display sensitivity to *Ovol* dosage by altering their gene expression and differentiation programs. Thus, this work adds *Ovol1/2* to the short list of transcription factors including *Tcf3*, *Lhx2*, *Sox9* and *Nfatc1* that regulate the behavior of adult HF-SCs. Interestingly, adult *Ovol2* SSKO mice show a slight delay in anagen entry with incomplete penetrance (data not shown), mirroring the premature progression to anagen observed in *Ovol2* BT mice. Further evidence that *Ovol* proteins are stem/progenitor cell-limiting factors to facilitate differentiation of adult HF-SCs awaits the generation of appropriate skin-specific *Ovol1/2*-deficient mouse models that do not exhibit perinatal lethality.

Our work mechanistically connects terminal differentiation, EMT, and cell adhesion of epidermal progenitor cells via an *Ovol*-*Zeb1*- α -catenin sequential-repression pathway. DKO epidermal cells share the α -catenin deficiency-induced defects in actin cytoskeletal organization and intercellular adhesion (Vasioukhin et al., 2001). Furthermore, like skin-specific *Cttna1* knockout, DKO mice show hyperproliferative epidermis and defective HF development. That *Ovol* regulation of α -catenin is mediated by *Zeb1* is particularly interesting. Although *Cdh1* has been extensively studied as a *Zeb1* target in cancer cells (Peinado et al., 2007), our data showcase α -catenin as the primary effector downstream of

Ovol and Zeb1 during epidermal morphogenesis. This function of mammalian Ovol, namely regulating actin cytoskeleton, is somewhat reminiscent of the role of *Drosophila* Ovo (Delon et al., 2003), but with an interesting molecular twist.

It is intriguing to ponder why an inducer of non-epithelial fate is built into the molecular circuit that promotes epithelial adhesion and differentiation. Dynamic changes associated with the adherens junctions provide flexible intercellular adhesions, with transient breakage and reestablishment of adhesive forces likely underlying the proliferative events within the epidermal stem/progenitor cell compartments and the migration of differentiating cells from basal to suprabasal locations (Kobielak and Fuchs, 2004; Watt, 1987). Our study demonstrates that this extremely mild form of epithelial plasticity during epidermal development shares some common molecular features and regulators, such as Ovol and Zeb1, with its more “radical” cousins, EMT and the reverse process MET (Ocana and Nieto, 2008; Roca et al., 2013). Moreover, Ovol repression of a plasticity inducer (Zeb1) that suppresses epithelial adhesion (α -catenin) seems a particularly “clever” strategy to ensure a delicate balance between adhesion relaxation and reestablishment. Supporting the broad relevance of this regulation, a spontaneous noncoding point mutation (*Twirler*) in the first intron of *Zeb1* that disrupts a conserved base pair within the +286 Ovol1/2 binding consensus (Figure 7A) results in inner ear defects (Kurima et al., 2011). Our findings raise the possibility that Zeb1 may normally function in developing epidermis as an adhesion relaxer. The presence of Zeb1 protein at the basal-suprabasal junction is consistent with this notion. Although examination of *Zeb1* null embryonic epidermis did not reveal any apparent anomaly (data not shown), it remains possible that *Zeb2* provides functional compensation.

EMT has recently been shown to promote stem cell properties (Chaffer et al., 2013; Guo et al., 2012; Mani et al., 2008). The fact that *Ovol1/2*-deficient epidermal cells are EMT-prone and “locked” in a proliferative progenitor state seems consistent with this. However, inhibition of EMT by *Zeb1* knockdown in *Ovol1/2* DKO keratinocytes does not decrease, but instead increases, colony formation. Thus, an epithelial fate is required for maximal clonogenicity, a surrogate measure of stem/progenitor activity of epidermal cells. *Ovol1/2* may also suppress proliferation potential via additional mechanisms independent of Zeb1, α -catenin, or EMT-like events, such as via regulating *Myc* and *p63*. Regardless, our discovery of Ovol involvement in suppressing both progenitor-like traits and epithelial plasticity paves the way for future studies of their potential role in cancer initiation and metastasis.

EXPERIMENTAL PROCEDURES

Mice

K14-Cre transgenic, floxed (f) and null (–) alleles of *Ovol2*, and *K5-tTA* mice have been described previously (Andl et al., 2004; Diamond et al., 2000; Indra et al., 2000; Unezaki et al., 2007). *TRE-Ovol2-Flag* transgenic founders were generated by pronuclei injection of CB6F1 mouse eggs at the University of California, Irvine (UCI) Transgenic Mouse Facility (TMF).

Immunostaining

For indirect immunofluorescence, mouse back skins were freshly frozen in OCT (Tissue Tek) and stained using the appropriate antibodies. The number of pH3⁺ cells was counted in at least 3 fields (using ImageJ of skin sections at 10x magnification) per mouse.

Immunohistochemical detection of p63 and Tcf3 was performed with paraformaldehyde-fixed OCT sections, using Vector ABC (Vector laboratories, PK-6100) and DAB (DAKO, K3468) kits per manufacturer's instructions.

Isolation of epidermis and culturing of primary keratinocytes

Skins of E18.5 embryos were placed with the dermis facing down in Petri dishes with 1 mL 5 mg/mL dispase (STEMCELL Technologies, 7913) and 1 mL CnT-07 media (CELLnTEC, CnT-07). Skins were incubated in the dispase/media solution at room temperature for 2–4 hours or overnight at 4°C. After incubation the dermis and epidermis are separated with forceps.

Keratinocytes were isolated from E18.5 skin of wild-type and mutant littermates using an established protocol (CELLnTEC). About 2–4×10⁶ cells were recovered from each mouse and were plated at comparable cell densities among genotypes. The cells were cultured in CnT-02 media (CELLnTEC, CnT-02) with or without addition of 1.2 mM Ca²⁺ for 3–5 days prior to experiments. For clonogenicity assay, cells were plated at 1000 cells/cm² and allowed to grow for two weeks, followed by staining with 0.5% Methylene blue and 50% ethanol for 30 minutes. For quantitative analysis, two wells of a six-well plate were counted and averaged per mouse.

ChIP assay

ChIP was performed according to the protocol described previously (Dahl and Collas, 2008) using primary keratinocytes isolated from newborn control embryos and cultured to reach 70%–80% confluency.

Microarray analysis

Hybridization of arrays (GeneChip Mouse Exon 1.0 ST Array, Affymetrix, Santa Clara, CA) was performed in duplicate using independent biological samples. Affymetrix GeneChip Analysis Suite software (MAS 5.0) was used to generate raw data and genes with normalized expression levels over detection threshold were called and analyzed for differential expression using the Cyber T program (Long et al., 2001) (<http://cybert.ics.uci.edu/>). The microarray data have been deposited into the GEO database (accession number GSE55075).

siRNA knockdown

Primary mouse DKO keratinocytes were reverse transfected in 6-well plates using LipofectamineTM RNAiMAX Transfection Reagent (Life Technologies, 13778-075) according to the manufacturer's recommendations. The following Silencer predesigned siRNAs (Life Technologies) were used at a concentration of 10–25 nM: Silencer® Select Negative Control No. 1 siRNA(4390843) and Zeb1 silencer select siRNA (4390771). Cells

were harvested 24–96 hours after transfection for RNA analysis or up to two weeks for morphological analysis.

Additional details for the above procedures, as well as procedures for histology, laser capture microdissection, RT-PCR, barrier, scratch and reporter assays, Western blotting, GSEA, and statistical analysis are described in the Supplemental Experimental Procedures.

Supplementary Material

Refer to Web version on PubMed Central for supplementary material.

Acknowledgments

We thank UCI Genomics High Throughput Facility and UCI TMF for service, Yoichiro Iwakura for help in generating *Ovol2* mutant alleles, Julie Segre, Hoang Nguyen, Douglas Darling, Valera Vasioukhin, and Leonard Milstone for antibodies, Sarah Millar for *K14-Cre* mice, and Adam Glick for *K5-tTA* mice. We thank Elaine Fuchs, Bogi Andersen and Kazuhide Watanabe for critical reading of the manuscript. This work was supported by NIH Grants R01-AR47320, R01-GM083089, K02-AR51482 (to X.D.), NIH Grants R01GM67247 and P50GM76516, NSF grant DMS-0917492 (to Q. N.), and NSF grant DMS-1161621 (to Q.N. and X.D.). Briana Lee was supported by the NIH Systems Biology of Development (T32HD060555) and NIH Translational Research in Cancer Genomic Medicine (T32CA113265) training grants. Jeremy Ovidia was supported by the Computational and Systems Biology (T32EB009418) and NIH Systems Biology of Development (T32HD060555) training grants.

ABBREVIATIONS

DKO	double knockout
DOX	doxycycline
E	embryonic day
Ecad	E-cadherin
EM	electron microscopy
EMT	epithelial to mesenchymal transition
GSEA	gene set enrichment analysis
HF	hair follicle
HG	hair germ
K	keratin
Ncad	N-cadherin
ORS	outer root sheath
P	postnatal day
SMA	smooth muscle actin
Vim	vimentin

References

Andl T, Ahn K, Kairo A, Chu EY, Wine-Lee L, Reddy ST, Croft NJ, Cebra-Thomas JA, Metzger D, Chambon P, et al. Epithelial *Bmpr1a* regulates differentiation and proliferation in postnatal hair

- follicles and is essential for tooth development. *Development*. 2004; 131:2257–2268. [PubMed: 15102710]
- Beck B, Blanpain C. Mechanisms regulating epidermal stem cells. *EMBO J*. 2012; 31:2067–2075. [PubMed: 22433839]
- Blanpain C, Fuchs E. Epidermal homeostasis: a balancing act of stem cells in the skin. *Nat Rev Mol Cell Biol*. 2009; 10:207–217. [PubMed: 19209183]
- Byrne C, Tainsky M, Fuchs E. Programming gene expression in developing epidermis. *Development*. 1994; 120:2369–2383. [PubMed: 7525178]
- Chaffer CL, Marjanovic ND, Lee T, Bell G, Kleer CG, Reinhardt F, D'Alessio AC, Young RA, Weinberg RA. Poised chromatin at the ZEB1 promoter enables breast cancer cell plasticity and enhances tumorigenicity. *Cell*. 2013; 154:61–74. [PubMed: 23827675]
- Dahl JA, Collas P. A rapid micro chromatin immunoprecipitation assay (microChIP). *Nature protocols*. 2008; 3:1032–1045.
- Dai X, Schonbaum C, Degenstein L, Bai W, Mahowald A, Fuchs E. The ovo gene required for cuticle formation and oogenesis in flies is involved in hair formation and spermatogenesis in mice. *Genes Dev*. 1998; 12:3452–3463. [PubMed: 9808631]
- Delon I, Chanut-Delalande H, Payre F. The Ovo/Shavenbaby transcription factor specifies actin remodelling during epidermal differentiation in *Drosophila*. *Mechanisms of development*. 2003; 120:747–758. [PubMed: 12915226]
- Descargues P, Sil AK, Sano Y, Korchynski O, Han G, Owens P, Wang XJ, Karin M. IKKalpha is a critical coregulator of a Smad4-independent TGFbeta-Smad2/3 signaling pathway that controls keratinocyte differentiation. *Proc Natl Acad Sci U S A*. 2008; 105:2487–2492. [PubMed: 18268325]
- Diamond I, Owolabi T, Marco M, Lam C, Glick A. Conditional gene expression in the epidermis of transgenic mice using the tetracycline-regulated transactivators tTA and rTA linked to the keratin 5 promoter. *The Journal of investigative dermatology*. 2000; 115:788–794. [PubMed: 11069615]
- Fuchs E. Scratching the surface of skin development. *Nature*. 2007; 445:834–842. [PubMed: 17314969]
- Fuchs E. Skin stem cells: rising to the surface. *J Cell Biol*. 2008; 180:273–284. [PubMed: 18209104]
- Fuchs E, Nowak JA. Building epithelial tissues from skin stem cells. *Cold Spring Harb Symp Quant Biol*. 2008; 73:333–350. [PubMed: 19022769]
- Gomis RR, Alarcon C, He W, Wang Q, Seoane J, Lash A, Massague J. A FoxO-Smad synexpression group in human keratinocytes. *Proc Natl Acad Sci U S A*. 2006; 103:12747–12752. [PubMed: 16908841]
- Guo D, Xu BL, Zhang XH, Dong MM. Cancer stem-like side population cells in the human nasopharyngeal carcinoma cell line cne-2 possess epithelial mesenchymal transition properties in association with metastasis. *Oncol Rep*. 2012; 28:241–247. [PubMed: 22552840]
- Indra AK, Li M, Brocard J, Warot X, Bornert JM, Gerard C, Messaddeq N, Chambon P, Metzger D. Targeted somatic mutagenesis in mouse epidermis. *Hormone research*. 2000; 54:296–300. [PubMed: 11595821]
- Jamora C, Fuchs E. Intercellular adhesion, signalling and the cytoskeleton. *Nature cell biology*. 2002; 4:E101–108.
- Jamora C, Lee P, Kocieniewski P, Azhar M, Hosokawa R, Chai Y, Fuchs E. A signaling pathway involving TGF-beta2 and snail in hair follicle morphogenesis. *PLoS Biol*. 2005; 3:e11. [PubMed: 15630473]
- Kalluri R, Weinberg RA. The basics of epithelial-mesenchymal transition. *J Clin Invest*. 2009; 119:1420–1428. [PubMed: 19487818]
- Kobielak A, Fuchs E. Alpha-catenin: at the junction of intercellular adhesion and actin dynamics. *Nat Rev Mol Cell Biol*. 2004; 5:614–625. [PubMed: 15366705]
- Koster MI, Dai D, Roop DR. Conflicting roles for p63 in skin development and carcinogenesis. *Cell Cycle*. 2007; 6:269–273. [PubMed: 17224652]
- Kurima K, Hertzano R, Gavrilova O, Monahan K, Shpargel KB, Nadaraja G, Kawashima Y, Lee KY, Ito T, Higashi Y, et al. A noncoding point mutation of Zeb1 causes multiple developmental malformations and obesity in Twirler mice. *PLoS Genet*. 2011; 7:e1002307. [PubMed: 21980308]

- Li B, Dai Q, Li L, Nair M, Mackay DR, Dai X. *Ovol2*, a mammalian homolog of *Drosophila ovo*: gene structure, chromosomal mapping, and aberrant expression in blind-sterile mice. *Genomics*. 2002a; 80:319–325. [PubMed: 12213202]
- Li B, Mackay DR, Dai Q, Li TW, Nair M, Fallahi M, Schonbaum CP, Fantes J, Mahowald AP, Waterman ML, et al. The LEF1/beta -catenin complex activates *movo1*, a mouse homolog of *Drosophila ovo* required for epidermal appendage differentiation. *Proc Natl Acad Sci U S A*. 2002b; 99:6064–6069. [PubMed: 11983900]
- Li B, Nair M, Mackay DR, Bilanchone V, Hu M, Fallahi M, Song H, Dai Q, Cohen PE, Dai X. *Ovol1* regulates meiotic pachytene progression during spermatogenesis by repressing *Id2* expression. *Development*. 2005; 132:1463–1473. [PubMed: 15716349]
- Lien WH, Guo X, Polak L, Lawton LN, Young RA, Zheng D, Fuchs E. Genome-wide maps of histone modifications unwind in vivo chromatin states of the hair follicle lineage. *Cell Stem Cell*. 2011; 9:219–232. [PubMed: 21885018]
- Long AD, Mangalam HJ, Chan BY, Tollerli L, Hatfield GW, Baldi P. Improved statistical inference from DNA microarray data using analysis of variance and a Bayesian statistical framework. Analysis of global gene expression in *Escherichia coli* K12. *J Biol Chem*. 2001; 276:19937–19944. [PubMed: 11259426]
- Mackay DR, Hu M, Li B, Rheaume C, Dai X. The mouse *Ovol2* gene is required for cranial neural tube development. *Dev Biol*. 2006; 291:38–52. [PubMed: 16423343]
- Maiden SL, Hardin J. The secret life of alpha-catenin: moonlighting in morphogenesis. *J Cell Biol*. 2011; 195:543–552. [PubMed: 22084304]
- Mani SA, Guo W, Liao MJ, Eaton EN, Ayyanan A, Zhou AY, Brooks M, Reinhard F, Zhang CC, Shipitsin M, et al. The epithelial-mesenchymal transition generates cells with properties of stem cells. *Cell*. 2008; 133:704–715. [PubMed: 18485877]
- Mills AA, Zheng B, Wang XJ, Vogel H, Roop DR, Bradley A. p63 is a p53 homologue required for limb and epidermal morphogenesis. *Nature*. 1999; 398:708–713. [PubMed: 10227293]
- Mootha VK, Lindgren CM, Eriksson KF, Subramanian A, Sihag S, Lehar J, Puigserver P, Carlsson E, Ridderstrale M, Laurila E, et al. PGC-1alpha-responsive genes involved in oxidative phosphorylation are coordinately downregulated in human diabetes. *Nature genetics*. 2003; 34:267–273. [PubMed: 12808457]
- Nair M, Bilanchone V, Ortt K, Sinha S, Dai X. *Ovol1* represses its own transcription by competing with transcription activator c-Myb and by recruiting histone deacetylase activity. *Nucleic Acids Res*. 2007; 35:1687–1697. [PubMed: 17311813]
- Nair M, Teng A, Bilanchone V, Agrawal A, Li B, Dai X. *Ovol1* regulates the growth arrest of embryonic epidermal progenitor cells and represses c-myc transcription. *J Cell Biol*. 2006; 173:253–264. [PubMed: 16636146]
- Nguyen H, Rendl M, Fuchs E. Tcf3 governs stem cell features and represses cell fate determination in skin. *Cell*. 2006; 127:171–183. [PubMed: 17018284]
- Nowak JA, Polak L, Pasolli HA, Fuchs E. Hair follicle stem cells are specified and function in early skin morphogenesis. *Cell Stem Cell*. 2008; 3:33–43. [PubMed: 18593557]
- Ocana OH, Nieto MA. A new regulatory loop in cancer-cell invasion. *EMBO Rep*. 2008; 9:521–522. [PubMed: 18483485]
- Payre F, Vincent A, Carreno S. *ovo/svb* integrates *Wingless* and *DER* pathways to control epidermis differentiation. *Nature*. 1999; 400:271–275. [PubMed: 10421370]
- Peinado H, Olmeda D, Cano A. Snail, Zeb and bHLH factors in tumour progression: an alliance against the epithelial phenotype? *Nat Rev Cancer*. 2007; 7:415–428. [PubMed: 17508028]
- Roca H, Hernandez J, Weidner S, McEachin RC, Fuller D, Sud S, Schumann T, Wilkinson JE, Zaslavsky A, Li H, et al. Transcription Factors *OVOL1* and *OVOL2* Induce the Mesenchymal to Epithelial Transition in Human Cancer. *PloS one*. 2013; 8:e76773. [PubMed: 24124593]
- Romano RA, Smalley K, Liu S, Sinha S. Abnormal hair follicle development and altered cell fate of follicular keratinocytes in transgenic mice expressing *DeltaNp63alpha*. *Development*. 2010; 137:1431–1439. [PubMed: 20335364]
- Shirley SH, Hudson LG, He J, Kusewitt DF. The skinny on Slug. *Mol Carcinog*. 2010; 49:851–861. [PubMed: 20721976]

- Teng A, Nair M, Wells J, Segre JA, Dai X. Strain-dependent perinatal lethality of *Ovol1*-deficient mice and identification of *Ovol2* as a downstream target of *Ovol1* in skin epidermis. *Biochim Biophys Acta*. 2007; 1772:89–95. [PubMed: 17049212]
- Thiery JP, Acloque H, Huang RY, Nieto MA. Epithelial-mesenchymal transitions in development and disease. *Cell*. 2009; 139:871–890. [PubMed: 19945376]
- Tinkle CL, Lechler T, Pasolli HA, Fuchs E. Conditional targeting of E-cadherin in skin: insights into hyperproliferative and degenerative responses. *Proc Natl Acad Sci U S A*. 2004; 101:552–557. [PubMed: 14704278]
- Unezaki S, Horai R, Sudo K, Iwakura Y, Ito S. *Ovol2/Movo*, a homologue of *Drosophila ovo*, is required for angiogenesis, heart formation and placental development in mice. *Genes Cells*. 2007; 12:773–785. [PubMed: 17573777]
- Vasioukhin V, Bauer C, Degenstein L, Wise B, Fuchs E. Hyperproliferation and defects in epithelial polarity upon conditional ablation of alpha-catenin in skin. *Cell*. 2001; 104:605–617. [PubMed: 11239416]
- Vasioukhin V, Bauer C, Yin M, Fuchs E. Directed actin polymerization is the driving force for epithelial cell-cell adhesion. *Cell*. 2000; 100:209–219. [PubMed: 10660044]
- Watt FM. Influence of cell shape and adhesiveness on stratification and terminal differentiation of human keratinocytes in culture. *Journal of cell science Supplement*. 1987; 8:313–326. [PubMed: 2460477]
- Wells J, Lee B, Cai AQ, Karapetyan A, Lee WJ, Rugg E, Sinha S, Nie Q, Dai X. *Ovol2* suppresses cell cycling and terminal differentiation of keratinocytes by directly repressing c-Myc and Notch1. *J Biol Chem*. 2009; 284:29125–29135. [PubMed: 19700410]
- Woo WM, Oro AE. SnapShot: hair follicle stem cells. *Cell*. 2011; 146:334–334. e332. [PubMed: 21784251]
- Yang A, Schweitzer R, Sun D, Kaghad M, Walker N, Bronson RT, Tabin C, Sharpe A, Caput D, Crum C, et al. p63 is essential for regenerative proliferation in limb, craniofacial and epithelial development. *Nature*. 1999; 398:714–718. [PubMed: 10227294]
- Yang J, Weinberg RA. Epithelial-mesenchymal transition: at the crossroads of development and tumor metastasis. *Dev Cell*. 2008; 14:818–829. [PubMed: 18539112]
- Zeller KI, Jegga AG, Aronow BJ, O'Donnell KA, Dang CV. An integrated database of genes responsive to the Myc oncogenic transcription factor: identification of direct genomic targets. *Genome Biol*. 2003; 4:R69. [PubMed: 14519204]

HIGHLIGHTS

- Inhibition of progenitor-like traits in skin epithelia requires Ovol1/2 proteins
- Ovol1/2 promote terminal differentiation in both epidermis and hair follicles
- Failure to restrict epidermal plasticity during development curtails differentiation
- Ovol-Zeb1- α -catenin pathway links plasticity control to adhesion and differentiation

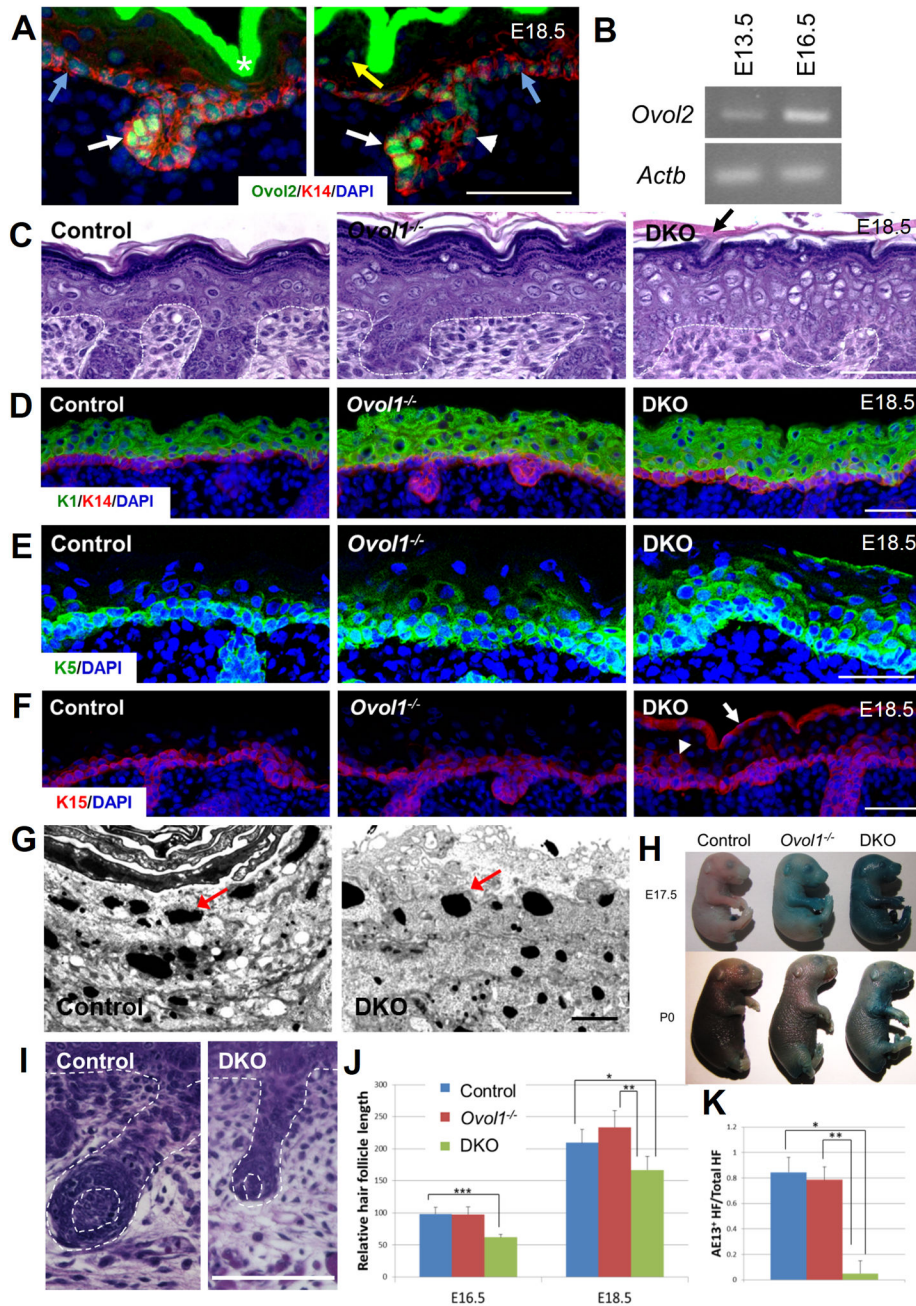


Figure 1. Loss of *Ovov1* and *Ovov2* results in defective epidermal and HF maturation
 (A) Indirect immunofluorescence of *Ovov2*. Gray and yellow arrows, basal and suprabasal cells, respectively. White arrows, anterior HF cells; arrowhead, presumptive outer root sheath (ORS) cells; white "*" indicates non-specific signals. (B) Semi-quantitative RT-PCR analysis of *Ovov2* mRNA at the indicated stages of development. *Actb* serves as a loading control. (C) Hematoxylin and eosin (H/E) staining. (D–F) Indirect immunofluorescence of the indicated markers. Arrows in C and F point to the periderm. Arrowhead in F indicates suprabasal cells that are K15-positive. DAPI stains the nuclei. (G) EM images of granular and cornified layers. Note that keratohyalin granules (red arrows) in DKO display a rounder, more electron-dense appearance compared to control. (H) Photographs of embryos at E17.5 and P0. (I) H/E staining of hair follicles. (J) Bar graph showing relative hair follicle length at E16.5 and E18.5. (K) Bar graph showing the ratio of AE13+ HF to total HF at E18.5.

less mature morphology. (H) Results of dye penetration assays. (I) Morphology of HFs at E18.5. (J) HF length (n = 2 and n = 4 per genotype for E16.5 and E18.5, respectively). * $p=0.01$, ** $p<0.02$, *** $p<0.004$. (K) Percent of HFs that are AE13-positive in E18.5 skin (n = 4 per genotype). Genotypes are as indicated in J. * $p<0.0001$, ** $p<0.02$. Error bars represent standard error. Bar: 25 μm in A, 50 μm in C–F, 2 μm in G, 50 μm in I. See also Figure S1.

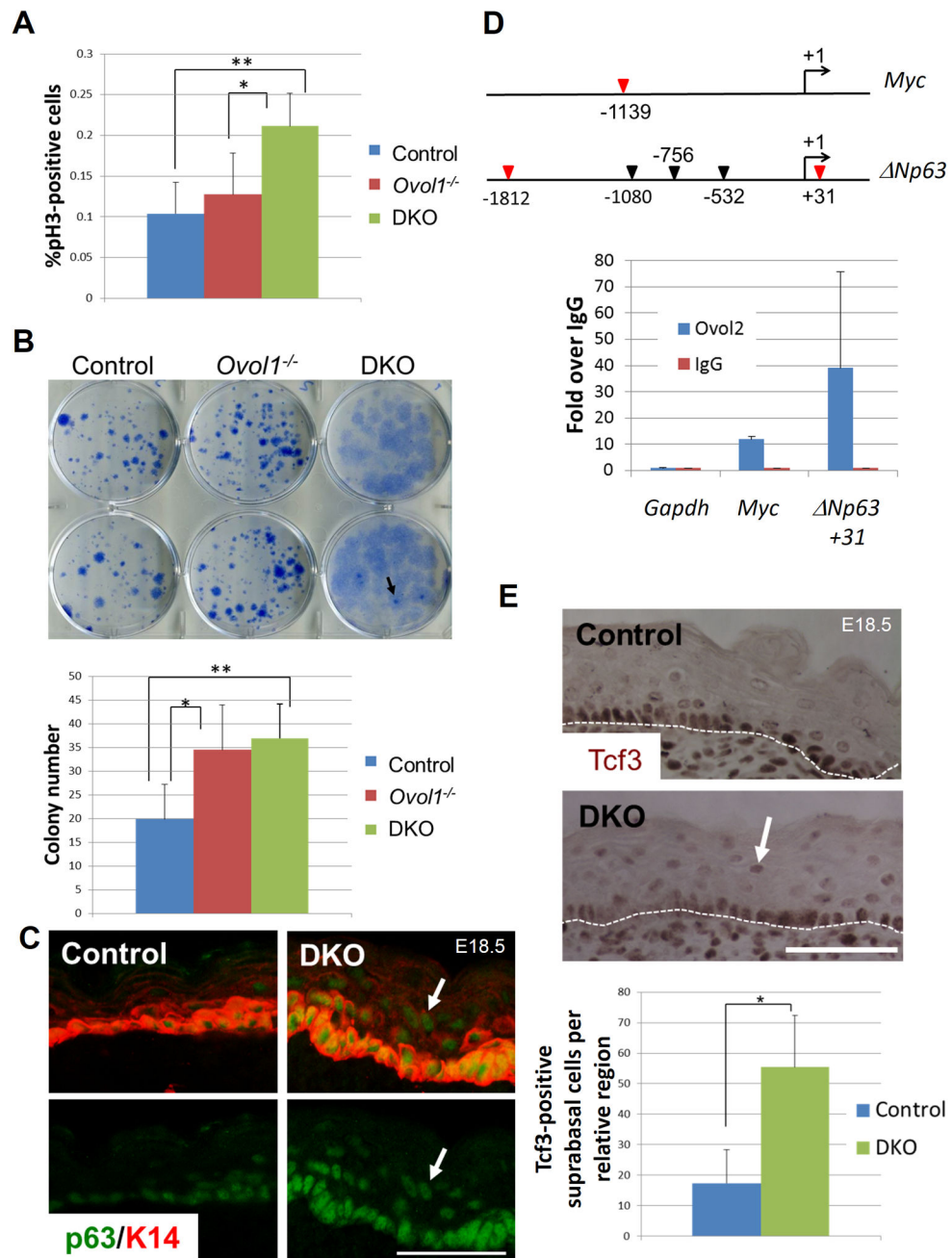


Figure 2. Increased proliferation and clonogenicity with loss of *Ovol1* and *Ovol2*
 (A) Basal cell proliferation. Shown are results of quantification of pH3-positive cells in skin of the indicated genotypes (n = 5 per genotype). * $p < 0.08$, ** $p < 0.0002$. (B) Morphology (top) and number (bottom) of colonies produced by keratinocytes from embryonic skin (n = 4 per genotype). Arrow points to a DKO colony with dense morphology at the center reminiscent of that in a typical epithelial colony, surrounded by loose, lightly stained peripheral cells. *, $p < 0.01$, ** $p < 0.0002$. (C) Immunofluorescent detection of p63. Top, merged images showing p63 and K14 double staining. Bottom, p63 only. Arrows point to p63-positive suprabasal cells in DKO epidermis. (D) ChIP analysis of *Ovol2* on *Myc* and *Np63* (diagrams shown at

the top). Triangles, putative Ovol sites, with validated binding sites shown in red. *Gapdh* serves as a negative control. (E) Immunohistochemical detection of Tcf3. Dashed line indicates the basement membrane. Arrow indicates aberrant suprabasal Tcf3⁺ cells (with their number quantified as shown at the bottom; n=4 per genotype). Error bars represent standard error. * $p=0.03$. Bar: 50 μm in C and E. See also Figures S2 and S3.

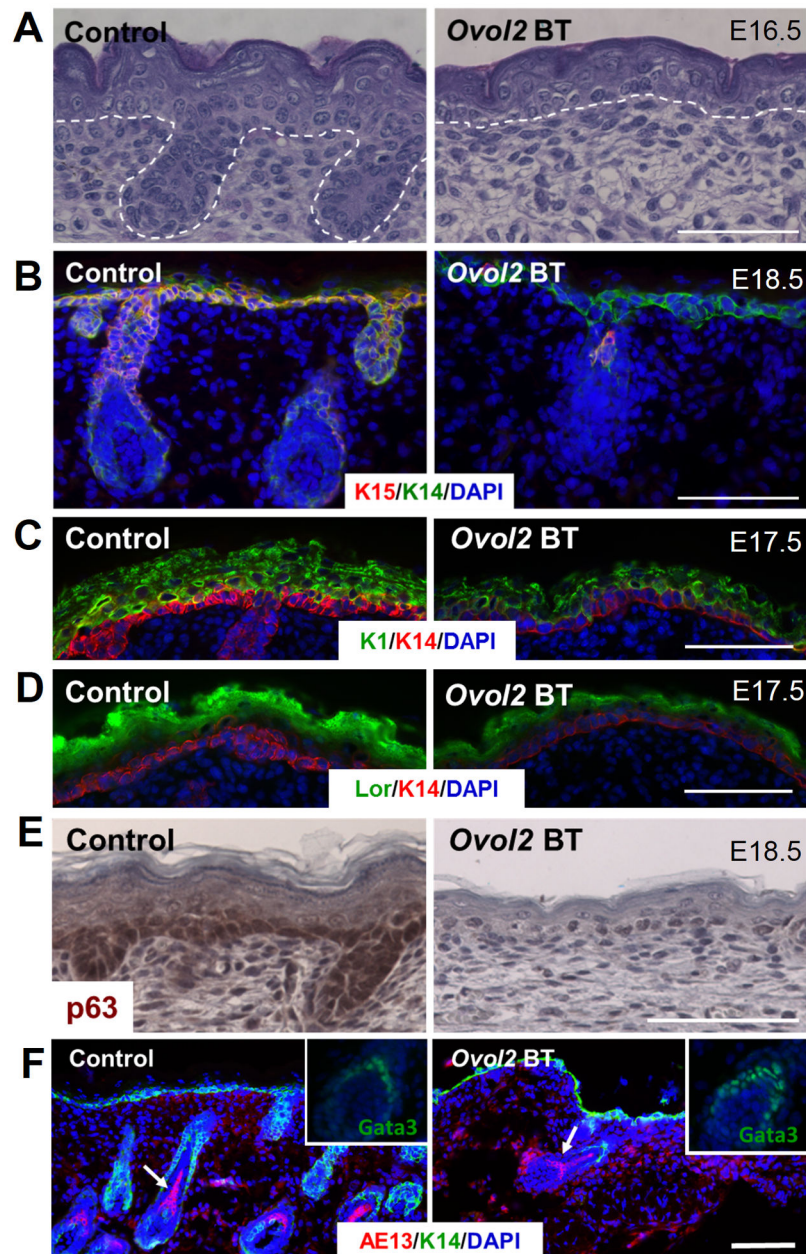


Figure 3. Skin phenotypes of *Ovo2* BT embryos

(A) H/E staining. (B–D, F) Indirect immunofluorescence of the indicated markers. Slides were double stained for K14, and nuclei were visualized by DAPI. (E) Immunohistochemistry using a pan-p63 antibody. Note the presence of AE13-positive cells (arrows in F) in a residual BT hair follicle. Gata3 staining images are shown as insets in F. Bar: 50 μ m in A–F. See also Figure S4.

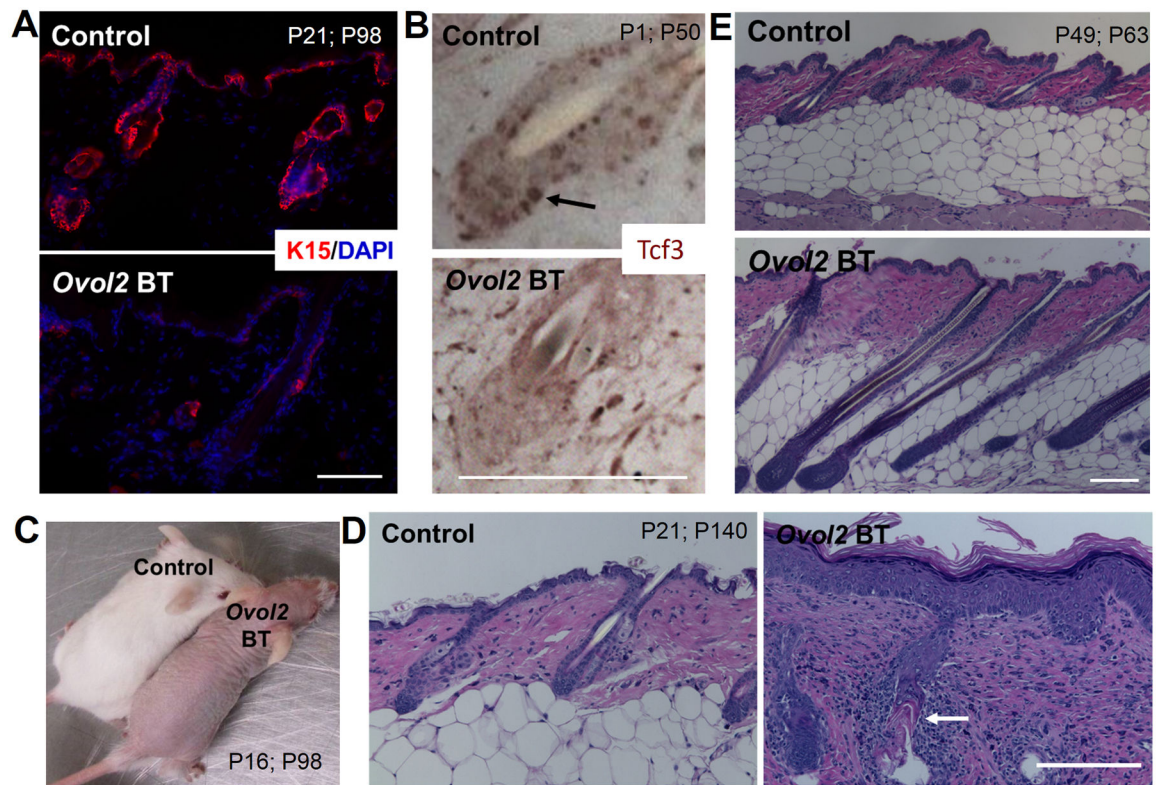


Figure 4. HF phenotypes of adult *Ovol2* BT mice

(A–B) Reduced presence of K15 (A) and Tcf3 (B) proteins in BT skin. Arrow in B indicates a Tcf3-positive secondary HG cell. (C–D) Long-term overexpression of *Ovol2* results in loss of hairs (C) and HFs (D). Arrow in D indicates the presence of epidermal-like materials in a residual HF. (E) Precocious progression of BT HFs to anagen. P₁; P₂ indicates the ages at which BT mice were induced with Dox and taken for analysis. Bar: 50 μ m in A–B, D, and 20 μ m in E. See also Figure S4.

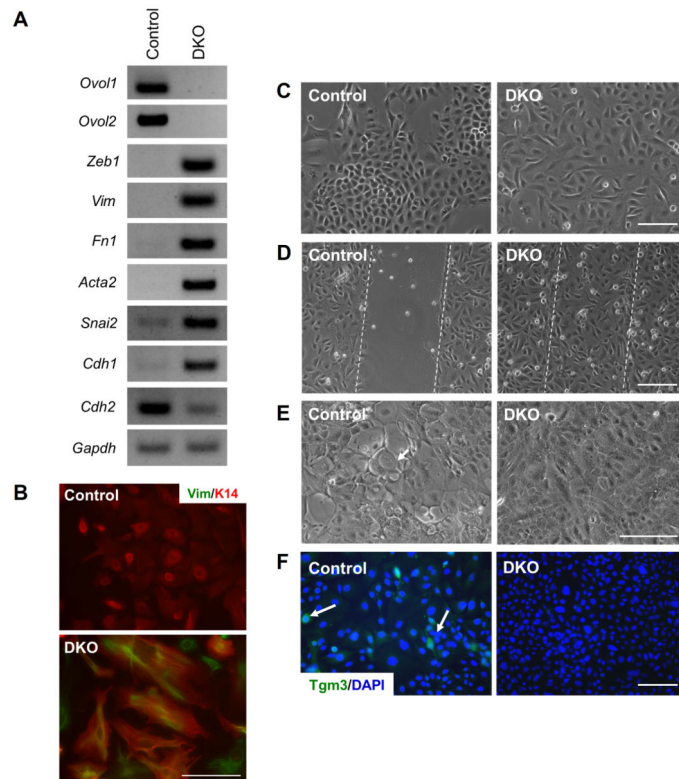


Figure 5. DKO epidermal keratinocytes undergo EMT-like molecular and morphological changes

(A) Semi-quantitative RT-PCR. *Gapdh* serves as a loading control. (B) Increased Vim protein expression in DKO keratinocytes. Shown are merged images with K14 staining. (C) Morphology of DKO keratinocytes in high-density culture. (D) Scratch assay. Dashed lines indicate where the scratches were made. (E) Morphology of Ca^{2+} -treated WT and DKO keratinocytes. (F) Indirect immunofluorescence of late epidermal differentiation marker transglutaminase 3 (Tgm3) in Ca^{2+} -treated keratinocytes. DAPI stains the nuclei. Arrows in E and F denote a large, flat differentiated cell and Tgm3-positive cells, respectively. Bar: 50 μ m in B–F. See also Figure S5.

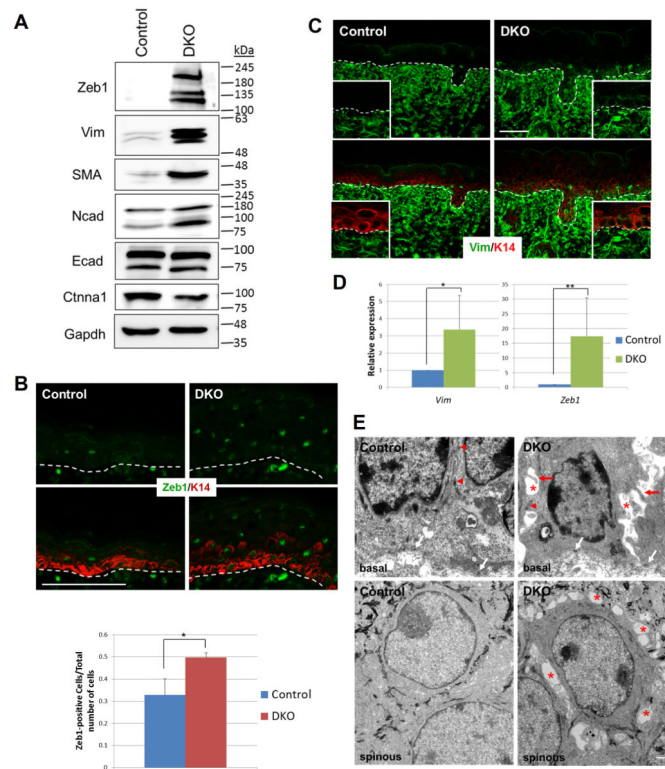


Figure 6. In vivo EMT-related changes in DKO epidermis

(A) Western blotting analysis of isolated epidermis. Gapdh serves as a loading control. Positions of molecular weight markers are indicated on the right. (B) Immunofluorescent detection of Zeb1 (top), with quantification of Zeb1-positive cells shown at the bottom ($n=3$ per genotype; *, $p<0.001$). Middle, merged images showing Zeb1 and K14 double staining. Note that many cells in the expanded K14-positive zone in DKO skin express Zeb1. (C) Immunofluorescent detection of Vim. Single channel (top) and merged (bottom, with K14) images are shown, with high magnification images included as insets. (D) RT-qPCR analysis of *Vim* and *Zeb1* mRNA levels in epidermis isolated from control and DKO skin. *, $p=0.109$, **, $p=0.096$. (E) EM images showing control and DKO basal (top) and spinous (bottom) cells. Red arrows, intercellular bridges; red arrowheads, desmosomes; red stars, intercellular gaps; white arrows, hemidesmosomes. Error bars represent standard error. Bar: 50 μm in B–C, 5.5 μm in upper panels and 1 μm in lower panels of E. See also Figure S5.

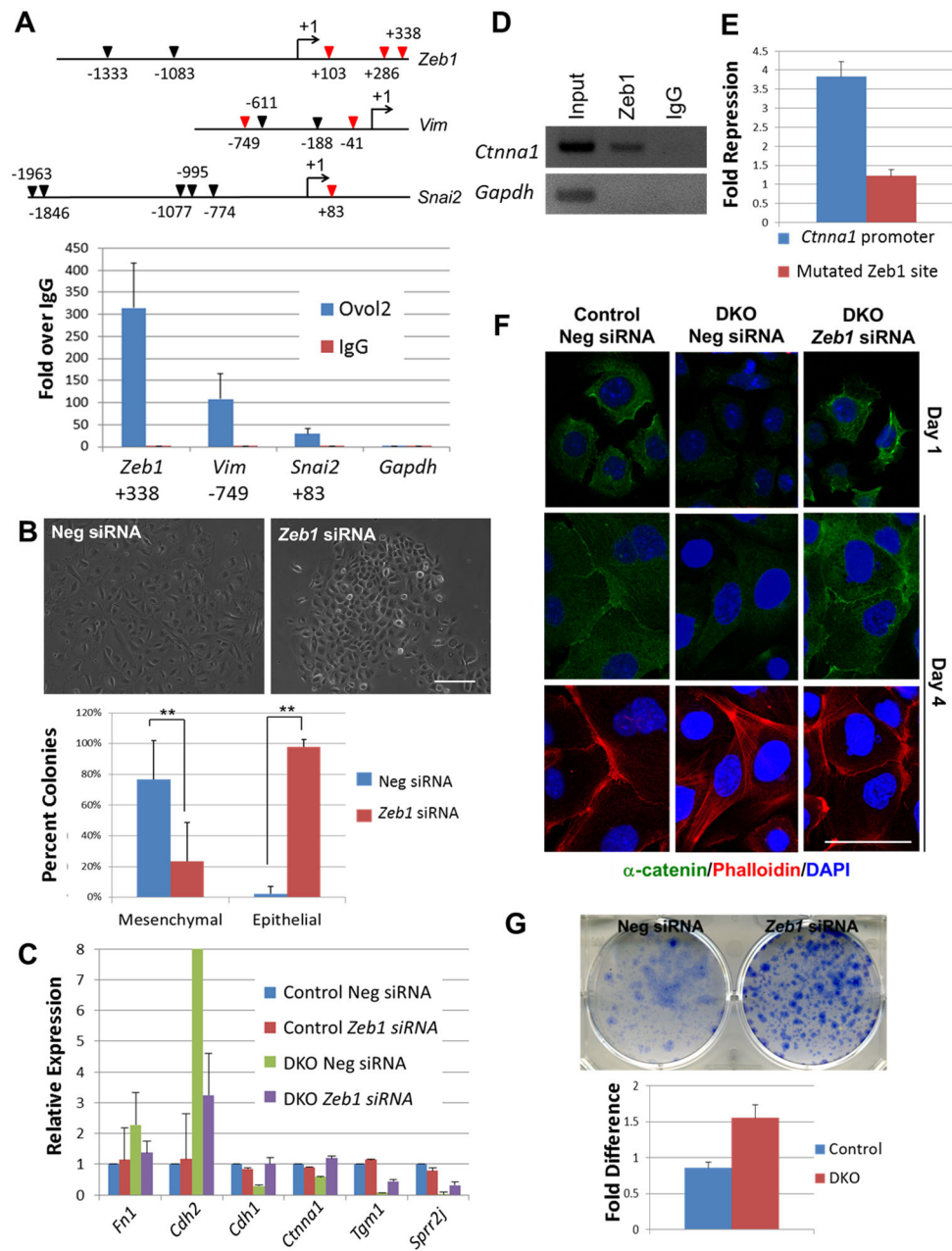


Figure 7. Evidence for an Ovol-Zeb1- α -catenin pathway and Zeb1 importance in *Ovol1/2* DKO phenotypes

(A) ChIP analysis of Ovol2 on *Zeb1*, *Vim* and *Snai2* (See legends to Figure 2D for more details). (B) Morphology (top) and type (bottom) of colonies produced by DKO keratinocytes treated with control (Neg) or *Zeb1* siRNA. **, $p < 0.0002$. (C) RT-qPCR analysis of Neg or *Zeb1* siRNA-treated keratinocytes. *Gapdh* expression was used for normalization. (D) ChIP revealing Zeb1 binding to *Ctnna1* promoter at predicted sites. The *Gapdh* promoter serves as a negative control. (E) WT but not mutated *Ctnna1* promoter is repressed by Zeb1 in luciferase reporter assays. (F) Indirect immunofluorescence of α -catenin and phalloidin on keratinocytes treated with Neg or *Zeb1* siRNA at the indicated

time points. Top and middle, merged images for α -catenin and DAPI. Bottom, merged images for phalloidin and DAPI. (G) Effect of *Zeb1* knockdown on keratinocyte clonogenicity. Graph depicts fold difference in the number of colonies comparing Neg control siRNA to *Zeb1* siRNA. Error bars represent standard error. Bar: 50 μ m in B and F. See also Figure S6.